energies

MDPI

Article

Coordinated Control of a Wind-Methanol-Fuel Cell System with Hydrogen Storage

Tiejiang Yuan [1], Qingxi Duan [1], Xiangping Chen [2,*], Xufeng Yuan [2], Wenping Cao [3], Juan Hu [4] and Quanmin Zhu [5]

1 Electrical Engineering School, Dalian University of Technology, Dalian 116024, China; ytj1975@dlut.edu.cn (T.Y.); dqx1991@163.com (Q.D.)
2 Electrical Engineering School, Guizhou University, Guiyang 550025, China; ee.xfyuan@gzu.edu.cn
3 School of Engineering & Applied Science, Aston University, Birmingham B4 7ET, UK; w.p.cao@aston.ac.uk
4 China Electric Power Research Institute, Beijing 102249, China; juanhoo@epri.sgcc.com.cn
5 Department of Engineering, Design and Mathematics, University of the West of England, Bristol BS16 1QY, UK; Quan.Zhu@uwe.ac.uk
* Correspondence: ee.xpchen@gzu.edu.cn

Received: 18 October 2017; Accepted: 30 November 2017; Published: 4 December 2017

Abstract: This paper presents a wind-methanol-fuel cell system with hydrogen storage. It can manage various energy flow to provide stable wind power supply, produce constant methanol, and reduce CO_2 emissions. Firstly, this study establishes the theoretical basis and formulation algorithms. And then, computational experiments are developed with MATLAB/Simulink (R2016a, MathWorks, Natick, MA, USA). Real data are used to fit the developed models in the study. From the test results, the developed system can generate maximum electricity whilst maintaining a stable production of methanol with the aid of a hybrid energy storage system (HESS). A sophisticated control scheme is also developed to coordinate these actions to achieve satisfactory system performance.

Keywords: coordinated control; energy storage; fuel cell; hydrogen; methanol production; wind power

1. Introduction

In order to curb global warming, international efforts have been devoted to developing renewable energy sources as well as utilizing conventional energy in a cleaner way. Wind energy, as a renewable source of energy, attracts much attention from research community and industry. As the largest CO_2 emitter, China had installed 150 million kW of wind turbines by the end of 2016 [1]. However, wind power is intermittent and its increasing penetration in the power network can create power stability issues. Therefore, much research is focused on the integration of wind energy in the power system for a resilient energy supply [2–5]. On the other hand, China is also the world's largest coal producer. Coal is a primary source of energy and accounts for 90% of China's CO_2 emissions from fossil fuels [6]. How to use coal in a cleaner way is always a challenge facing the successive Chinese governments.

Methanol is a clean-burning liquid that requires only minor modifications to existing engines and fuel-delivery infrastructure. Manufacturing it could even make use of carbon dioxide, which is the main cause for global warming. While methanol's benefits have long been understood, recent advances in methanol synthesis and methanol fuel cells could make this fuel even more attractive [7]. Conventionally, methanol is a by-product of mining coal through a hydrocarbylation reaction. In this process, 1.526 times of CO_2 could be produced with one unit of methanol. This has led to a significant increase in CO_2 emissions to the environment. In order to tackle this issue, a new representative process has been developed [8] to produce methanol from hydrogen, oxygen and coal which is used in this study.

Energy storage is important to maintain the stable operation of energy systems. Reference [9] presented a new energy storage design to support energy flow in a hybrid wind-hydrogen system. Reference [10] proposed a hybrid energy system consisting of a wind turbine generator, a fuel cell with a water electrolyser and a battery energy storage system. Typically, these energy components are divided into two groups and two PI controllers were used to manage energy flow. By combining wind energy with fuel cells, reference [11] discussed the feasibility of a hybrid system satisfying residential demands when connected to the power grid. Reference [12] proposed an optimal method for sizing a grid-connected wind farm with a hydrogen system. Fuel cell systems with wind energy were also investigated in references [13–16] in order to find an optimal structure in the hybrid system. New concepts for optimal applications for wind energy were proposed [17,18]. These hybrid energy systems were integrated with integrating wind energy and coal-based methanol production, so as to provide an effective method to utilize local energy resources. Energy management and control methods in multi energy sources are critically important also important. Fuzzy logic control is a popular option for hybrid energy systems. Reference [19] presented a particle swarm-based fuzzy logic control for a hybrid wind-fuel cell-battery system to decrease total harmonic distortion of the power sources. A maximum power point tracking (MPPT) algorithm was used in a wind-fuel cell system [20] to meet variable load. Reference [21] adopted a probability distribution function to manage a wind-fuel cell-turbine with energy storage. The test results for different scenario of load or demand uncertainty. These systems are effective but have their limitations. It is the author's review that using systematic approaches to integrate the developed techniques will increase multiple functions in the loop of energy generation, utilization, operation, clean environment and so on.

The research project uses Xinjiang, the large territory province in China, as a case background. It is an important energy base in China, it connects advanced provinces in East China eastward, and links to the Central Asia countries westward. Xinjiang is regarded as a strategic hub on the "Silk Road Economic Belt". It is rich in coal resources and wind energy, which is a perfect match for the project as generated electricity from wind can be used for water electrolysis to produce hydrogen and oxygen. Xinjiang has been one of the five national integrated energy bases [22,23]. Therefore, how to effectively utilise coal sources and wind energy in Xinjiang is one of the crucial issues in China's national agenda. In national perspective, China has been a major contributor to global warming and thus is committed to play a significant role to cut down its CO_2 emissions. In June 2014, China proposed a radical measure for managing its energy consumption and for developing renewable energy technologies. China has become the largest renewable producer in 2016, according to British Petroleum Statistical Review of World Energy [24].

This study proposes a hybrid system including a wind turbine, hydrogen/oxygen storage tanks through water electrolysis, a coal-base methanol device and a fuel cell. In this multi-source system, energy is managed into different forms: kinetic energy in a turbine; chemical energy in hydrogen/oxygen and fuel cells; electrical energy in the wind turbine/generators and the fuel cells. The hydrogen production through water electrolysis and the charging/discharging of the fuel cells provide flexibility when the intermittent wind power cannot match the energy requested. Meanwhile, methanol production with the new technology reduces the CO_2 emission for the system [17,25] which also in turn increase the revenue from the carbon trading scheme according to the national policy [26,27]. In this system, energy flow is managed by a coordinated control strategy. It determines the electricity generation and methanol production, with a target of maximising utilisation of wind energy. The feasibility and the performance of the strategy are tested through modeling and simulation in the MATLAB/Simulink environment. The novelty and contribution of the study are listed below.

(1) Integration wind energy into the grid has resulted in degradation of the inertia response, which in turn seriously affects the stability of the power system's frequency. This problem can be solved by

using an active power reserve to stabilize the frequency. Hydrogen/oxygen fuel cell technology is one of solution as a power reserve for this purpose.

(2) Hydrogen/oxygen production from water electrolysis could provide the resource for fuel cell applications. As typical electricity-to-hydrogen conversion devices, electrolysers are regarded as deferrable loads with the ability to operate under a flexible schedule on the demand side.

(3) The coal-based methanol production is one of research challenges of clean energy applications of fossil fuels. This study adopts a "greener" process. The oxygen is fed to the gasifier as the gasification agent and then the hydrogen is mixed with the CO-rich gas to adjust H_2/CO so as to produce methanol. However, it requires local supplies of hydrogen/oxygen continuously. Therefore, this kind of applications are limited. However, specific geometry advantages of Xinjiang province is perfect for this kind of applications.

(4) This innovative application integrates wind power, hydrogen from water electrolysis, hydrogen/oxygen fuel cells and a coal-based methanol production by a "greener" process. The system proposed has advantages of both the renewable sources and sustainable coal industries in China. Methanol receives hydrogen/oxygen to balance the local loads and to increase the overall profits. However, the hybrid construct would increase the system complexity. Therefore, it is necessary to investigate the possible energy management strategy and control mechanism before physical complicated system is build up.

The rest of the main studies are arranged as follows: Section 2 introduces the configuration of the hybrid system; Detailed discussion associated with the control scheme is carried out for energy management of this system; Section 3 provides the simulation outcomes and analysis; Section 4 summarises the main findings and suggests future work.

2. The Hybrid System and Its Control Scheme

The schematic diagram of the system is shown in Figure 1. The system includes a doubly-fed induction generator (DFIG) of a wind turbine, coal-based methanol production sub-system, a water electrolyser for hydrogen production, hydrogen and oxygen storage tanks, fuel cells, a DC link, DC/AC or AC/DC converters. The coal chemical process comprises gasification, mixing, purification, reaction, separation and rectification.

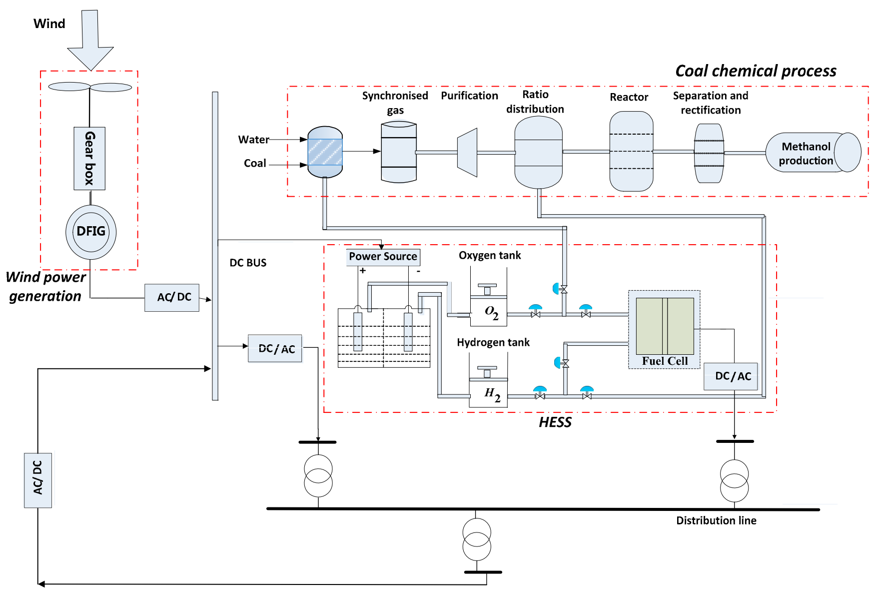

Figure 1. Schematic diagram of the proposed system.

This system is operated on the following basis:

i. Wind power is used to generate electricity for supplying the grid and for producing hydrogen through water electrolysis.
ii. Normally, the generated electricity is fed into the power grid. If the wind power is plenty, the additional power is used for water electrolysis and the energy is stored in hydrogen.
iii. Hydrogen and oxygen produced are stored in separate tanks and are controlled to be within a range (upper limit 90% and lower limit 20%).
iv. Fuel cells absorb hydrogen and generate electricity to supply the grid.
v. Methanol is produced constantly (from coal, hydrogen and oxygen) at a set value regardless of wind power input.

Figure 2 shows the operation of the proposed system.

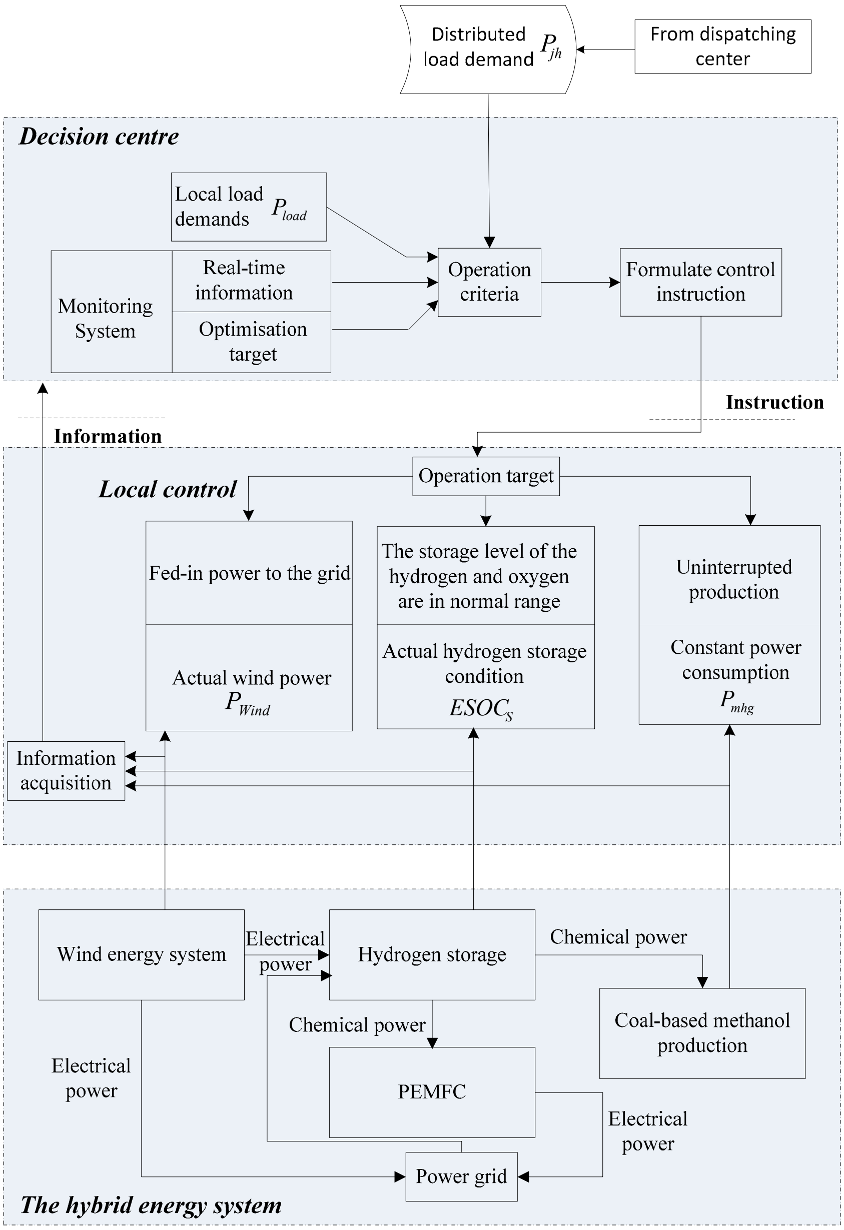

Figure 2. The proposed scheme with coordinated control.

2.1. State Index of the Hybrid Energy Storage System (HESS)

In this paper, the HESS consists of a water electrolyser, a hydrogen and an oxygen tank, and fuel cells. The energy flow in the HESS is bi-direction. However, methanol production is single direction and cannot be fed back. Therefore, coal-based methanol production is not involved in the storage system in this study. In the HESS, the equivalent state of charge (ESOC) is evaluated by the state of the hydrogen and oxygen tanks:

$$ESOC = \frac{p_{vre}}{p_{cap}} \tag{1}$$

where p_{vre} and p_{cap} are the current pressure and full pressure of the tanks, respectively. Based on the average weighting method, the $ESOC$ is calculated as follows:

$$ESOC_H = \frac{p_{Hre}}{p_{Hcap}} \tag{2}$$

$$ESOC_O = \frac{p_{Ore}}{p_{Ocap}} \tag{3}$$

$$ESOC_S = \frac{ESOC_H \times V_{Hcap} + ESOC_O \times V_{Ocap}}{V_{Hcap} + V_{Ocap}} \tag{4}$$

where $ESOC_H$ is the $ESOC$ level of the hydrogen storage tank, p_{Hre} is the pressure of the hydrogen tank, p_{Hcap} is the full pressure of the hydrogen tank, $ESOC_O$ is the $ESOC$ level of the oxygen tank, p_{Ore} is the pressure of the oxygen tank, p_{Ocap} is the full pressure of the oxygen tank, V_{Hcap} and V_{Ocap} are the volumes of hydrogen and oxygen tanks, respectively.

In order to operate the HESS effectively, the indicators of $ESOC_H$, $ESOC_O$, $ESOC_S$ should be controlled within reasonable range. Basically, they are divided into two intervals and three situations, as shown in Figure 3. Each interval can be determined by Equation (5):

$$\begin{cases} Normal \quad interval: ESOC_{X\_\min} \leq ESOC_X \leq ESOC_{X\_\max}, N_{H_2O} = N_{fc} + N_{mhg} \\ Warning \quad interval: \begin{cases} ESOC_X < ESOC_{X\_\min}, N_{H_2O} > N_{fc} + N_{mhg}, X = H, O, S \\ ESOC_X > ESOC_{X\_\max}, N_{H_2O} < N_{fc} + N_{mhg} \end{cases} \end{cases} \tag{5}$$

where $ESOC_{X\_\min}$ represents the minimal of $ESOC$ and X represents hydrogen, oxygen and HESS states, respectively. $ESOC_{X\_\max}$ is the maximal of hydrogen, oxygen and HESS. N_{H_2O} is the hydrogen flow rate in water electrolyser. N_{fc} is the hydrogen flow rate in the fuel cell. N_{mhg} is the hydrogen flow rate used in coal chemical system when producing methanol.

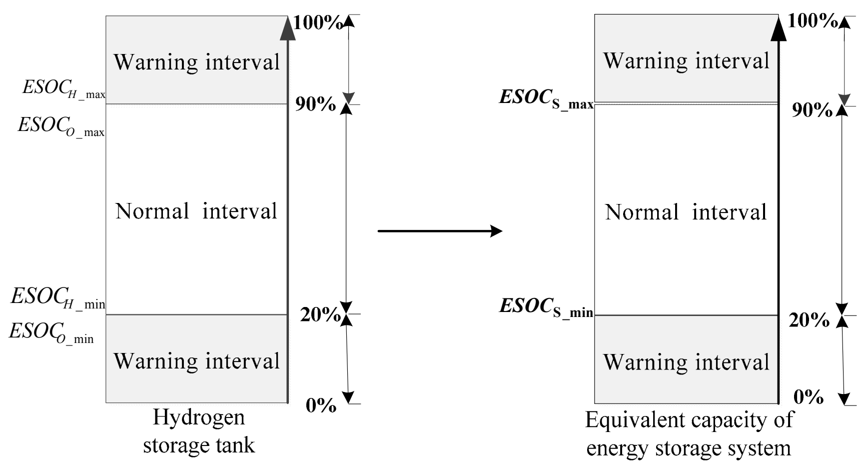

Figure 3. The capacity range of the HESS.

When the tank or $ESOC$ level is in the normal range, the coal chemical system operates normally to produce methanol. The ideal operation state of the system is that hydrogen generated by the water electrolysis is equal to the sum of hydrogen consumption in the methanol production and in the fuel cells discharging while the $ESOC$ of the HESS is still within the normal range.

In the control scheme, $ESOC_S$ is considered as the priority factor in the operation. And the relationship among the wind power output P_{wind}, the cluster power dispatch demand P_{jh}, local load demand P_{load} is defined as follows:

(1) When $ESOC_S > ESOC_{S\_\max}$, let $i = 1$ and $P_{re}^{(i)} = P_{wind} - \left(P_{load} + P_{jh}\right)$
(2) When $ESOC_{S\_\min} \leq ESOC_S \leq ESOC_{S\_\max}$, let $i = 2$ and $P_{re}^{(i)} = P_{wind} - P_{load}$
(3) When $ESOC_S < ESOC_{S\_\min}$, let $i = 3$ and $P_{re}^{(i)} = P_{wind}$

2.2. Operation Scheme of the Hybrid System

The system converts energy between electrical, chemical and mechanical. Hydrogen/oxygen generation is an integral part of the energy flow. The processes involve several reactions as follows [28,29]:

Water electrolysis: $H_2O \to \frac{1}{2}O_2 + 2H^+ + 2e^-$, therefore, $n(H_2)$:$n(O_2)$ = 2:1

Coal based methanol production: $CO + 2H_2 = CH_3OH$, therefore:

$$n(H_2) : n(O_2) = 1 : 1 \tag{6}$$

Electrochemical reactions in a fuel cell: $H_2 + \frac{1}{2}O_2 \to H_2O$, therefore, $n(H_2)$:$n(O_2)$ = 1:0.5

For the constant production of methanol at set power P_{mhg}, the hydrogen and oxygen are the same. The flow rate of hydrogen N_{mhg} and power demand $P_{re}^{(i)}$ are given in Table 1.

Table 1. Interval scheme of power $P_{re}^{(i)}$ with the flow rate N_{H_2}.

	fl$_1$	**fl**$_2$	**fl**$_3$	**fl**$_4$
$P_{re}^{(i)}$	$(0, P_{mhg})$	$[P_{mhg}, 2P_{mhg}]$	$(2P_{mhg}, 4P_{mhg}]$	$(4P_{mhg}, +\infty)$
N_{H_2}	$(0, N_{mhg})$	$[N_{mhg}, 2N_{mhg}]$	$(2N_{mhg}, 4N_{mhg}]$	$(4N_{mhg}, +\infty)$

When P_{H_2O} and N_{H_2O} are in interval γ_1, hydrogen from water electrolysis is not sufficient to sustain the required methanol production, as a result, the stored hydrogen in the tank is also consumed and $ESOC_S$ slowly reduces. When P_{H_2O} and N_{H_2O} are in interval γ_2, the generated hydrogen is more than the needed for methanol. Extra hydrogen is consumed by fuel cells to generate electricity. In γ_3 or γ_4, when the hydrogen is much more than needed, extra hydrogen is used for fuel cells and methanol and increasing tank levels. Table 2 gives detailed explanations.

Table 2. Operational regulation for different scenarios.

Indicator		**Scenario**	**Action**
$i = 1$ $P_{re}^{(i)} = P_{wind} - \left(P_{load} + P_{jh}\right)$	$P_{re}^{(i)} < 0$	$ESOC_S$ is over the upper limit. The wind power is insufficient to satisfy both local demands and cluster power requested by the grid.	The total wind power is fed into the grid. The fuel cells discharge. Water electrolysis suspends, $P_{H_2O} = 0$.
	$P_{re}^{(i)} = 0$	$ESOC_S$ is over the upper limit. The wind power is sufficient to satisfy both local and cluster power, the rest of the wind power is equal to 0.	The wind power is completely transferred to the grid. Water electrolysis suspends, $P_{H_2O} = 0$.
	$P_{re}^{(i)} \in Y_1$	$ESOC_S$ is over the upper limit. The wind power is sufficient to satisfy both local and cluster power. The rest of the wind power is within Y_1.	The wind power fed into the grid is set $(P_{load} + P_{jh})$, $P_{H_2O} = P_{re}^{(i)}$.

Table 2. *Cont.*

Indicator		Scenario	Action
	$P_{re}^{(i)} \in (Y_2 \cup Y_3 \cup Y_4)$	$ESOC_S$ is over the upper limit. The wind power is sufficient to satisfy both local and cluster power. The rest of the wind power is within Y_2 or Y_3 or Y_4.	The wind power is used for water electrolysis which provide the hydrogen for methanol production. P_{H_2O} = $P_{re}^{(i)}$ and the rest wind power is transferred to the grid.
$i = 2$ $P_{re}^{(i)} = P_{wind} - P_{load}$	$P_{re}^{(i)} < 0$	$ESOC_S$ is within the normal range. The wind power is insufficient to satisfy the local demands.	The total wind power is fed into the grid. The fuel cells discharge with P_{fc} = $\lvert P_{re}^{(i)} \rvert$. Water electrolysis process suspends, P_{H_2O} = 0.
	$P_{re}^{(i)} \in (Y_1 \cup Y_2)$ or $P_{re}^{(i)} \in (Y_3 \cup Y_4)$	$ESOC_S$ is within the normal range. The wind power is sufficient to satisfy the local demands. The rest of the wind power is within $(Y_1 \cup Y_2)$ or $(Y_3 \cup Y_4)$.	The fuel cells suspend. Wind power is used for water electrolysis which provide the hydrogen for methanol production with P_{H_2O} = $\lvert P_{re}^{(i)} \rvert$ or P_{H_2O} = $2P_{mhg}$. The rest wind power is fed to the grid.
$i = 3$ $P_{re}^{(i)} = P_{wind}$	$P_{re}^{(i)} = 0$	$ESOC_S$ is below the lower limit. No wind power provided.	Both The fuel cell and water electrolysis process suspend; No wind power is fed to the grid.
	$P_{re}^{(i)} \in (Y_1 \cup Y_2 \cup Y_3)$	$ESOC_S$ is below the lower limit. The wind power is within $(Y_1 \cup Y_2 \cup Y_3)$.	All wind power is used for water electrolysis P_{H_2O} = $P_{re}^{(i)}$.
	$P_{re}^{(i)} \in Y_4$	$ESOC_S$ is below the lower limit. The wind power is within Y_4.	The wind power used for water electrolysis P_{H_2O} is equal to $4P_{mhg}$. The rest wind power is fed to the grid.

2.3. Electrical Power and ESOC Control

Based on the control priority and the operating state of the system, a power distribution strategy is proposed. Its flow chart is shown in Figure 4. The power consumed by water electrolysis is obtained as follows:

$$P_{H_2O} = \begin{cases} 0 \; P_{re}^{(i)} \leq 0 \\ P_{re}^{(i)} \; 0 < P_{re}^{(i)} \leq 2^{(i-1)} P_{mhg} \\ 2^{(i-1)} P_{mhg} \; P_{re}^{(i)} \leq 2^{(i-1)} P_{mhg} \end{cases} \tag{7}$$

The fed-in wind power to the grid is given by:

$$P_S = P_{wind} - P_{H_2O} \tag{8}$$

All hydrogen is generated by water electrolysis and is consumed by either fuel cells or methanol production. Thus, the hydrogen distribution can be expressed by:

$$\begin{cases} n_{H_2O\_H} + n_{\Delta H} = n_{mhg\_H} + n_{rH} \\ n_{H_2O\_O} + n_{\Delta O} = n_{mhg\_O} + n_{rO} \end{cases} \tag{9}$$

where $n_{H_2O\_H}$ and $n_{H_2O\_O}$ are the amount of the hydrogen and oxygen produced by electrolysis of water respectively. $n_{\Delta H}$ and $n_{\Delta O}$ are the amount of the hydrogen and oxygen consumed in the tank respectively. n_{rH} and n_{rO} are the amount of hydrogen and oxygen that fed into the fuel cell respectively.

The hydrogen flow rate N_{H_2} from the electrolysis of water power P_{H_2O} is obtained:

$$N_{H_2} = \eta_e N_e \frac{I_e}{2F} = \eta_e N_e \frac{P_{H_2O}/N_e U_e}{2F} = \frac{\eta_e P_{H_2O}}{2U_e F} \tag{10}$$

where η_e is the electrolysis efficiency of water electrolyser, which is generally between 60% and 80% [30]. N_e is the number of electrolytic cells in series. F is the Faraday constant. Ie is the operating current of the cell which is given by dividing the consumption power P_{H_2O} by the electrolyser voltage Ue.

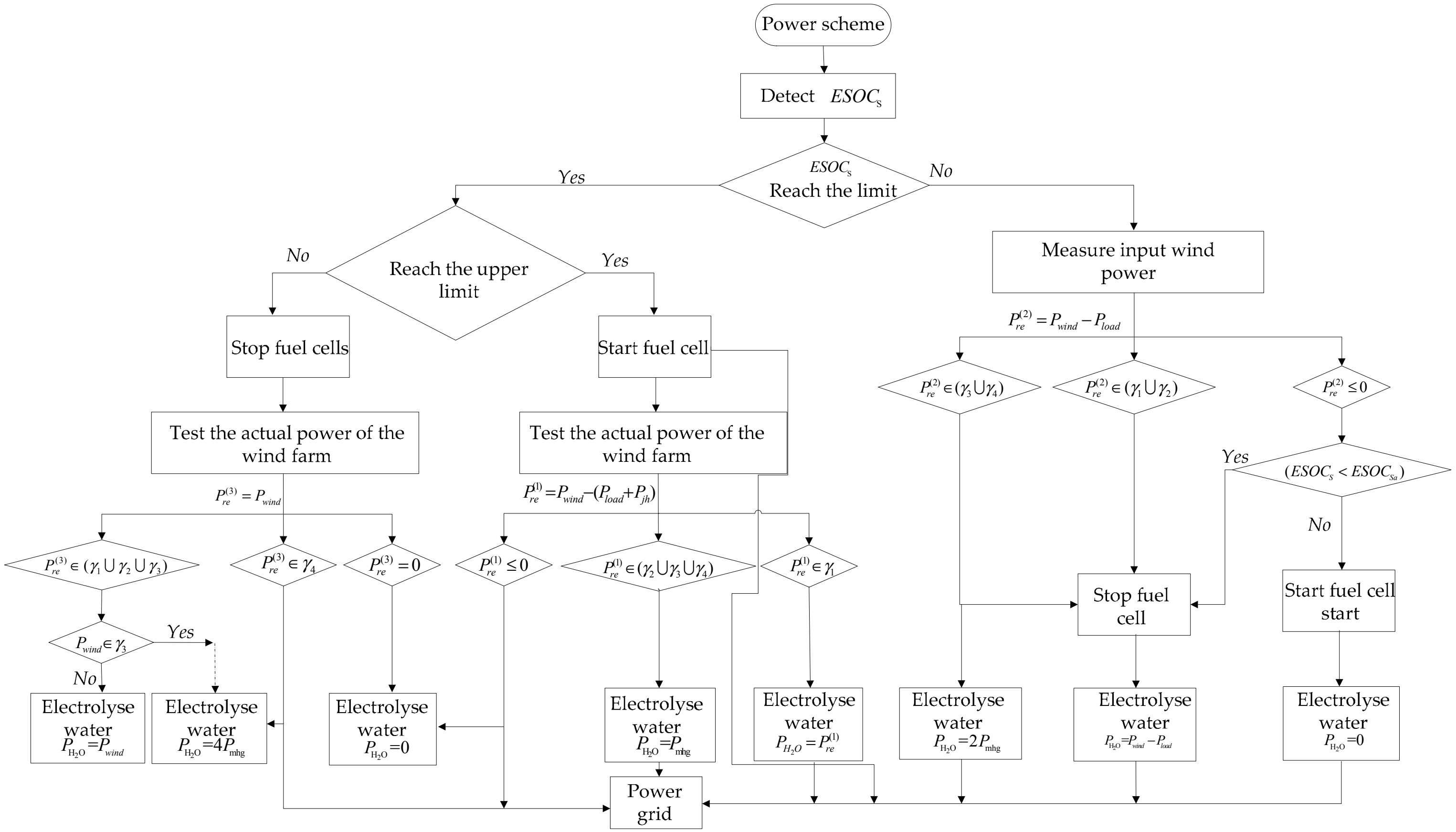

Figure 4. Control diagram of electric energy allocation.

Thus:

$$\begin{cases} n_{H_2O\_H} = N_{H_2}\Delta t \\ n_{H_2O\_O} = 0.5n_{H_2O\_H} = 0.5N_{H_2}\Delta t \end{cases} \tag{11}$$

Assuming the operation process is ideal, the amount of hydrogen and oxygen consumed in the coal chemical system during Δt can be written as:

$$n_{mhg\_H} = n_{mhg\_O} = N_{mhg} \times \Delta t \tag{12}$$

$$N_{mhg} = 207 \times 0.2 \times \frac{M_W}{3.6V_m} \tag{13}$$

where M_W is the wind turbine output power (MW), and V_m is the hydrogen molar volume 22.4 L/mol.

From Equation (8), n_{rO} can be derived from $n_{\Delta H}$ and $n_{\Delta O}$, and vice versa. Thereby the state of the hydrogen storage system at the end of each cycle can be obtained. Therefore, the hydrogen distribution control is simplified to study the operation state of the fuel cells. The cases for the fuel cells discharging can be summarised as the follows:

(1) If $P_{re}^{(1)} \geq 0$, reduce $ESOC_S$ by consuming more hydrogen and oxygen for electricity generation, Let flag1 = 1. Logical order is to derive n_{rH}, $n_{rO}(P_{fc})$ from $n_{\Delta H}$, $n_{\Delta O}$.

At this moment, the amount of hydrogen and oxygen can reach the upper limits of the tank pressure $n_{\Delta H}$, $n_{\Delta O}$:

$$\begin{cases} n'_{\Delta H} = p_{Hcap}\mathrm{V}_{Hcap}(ESOC_H - ESOC_{H\_\max})/\mathrm{RT}_H \\ n'_{\Delta O} = p_{Ocap}\mathrm{V}_{Ocap}(ESOC_O - ESOC_{O\_\max})/\mathrm{RT}_O \end{cases} \tag{14}$$

The calculations of the parameters $n_{\Delta H}$, $n_{\Delta O}$ are shown in Table 3.

Table 3. Parameter selection for the calculation.

$n'_{\Delta \mathrm{H}}$ / $n'_{\Delta \mathrm{O}}$	**<0**	**=0**	**>0**
<0	-	-	select $n_{\Delta \mathrm{H}} = n'_{\Delta \mathrm{H}}$
=0	-	-	select $n_{\Delta \mathrm{H}} = n'_{\Delta \mathrm{H}}$
>0	Select $n_{\Delta \mathrm{O}} = n'_{\Delta \mathrm{O}}$	Select $n_{\Delta \mathrm{O}} = n'_{\Delta \mathrm{O}}$	$\begin{cases} n_{\Delta H} = n'_{\Delta H} & if\ n'_{\Delta H} \geq 2.3n'_{\Delta O} \\ n_{\Delta O} = n'_{\Delta O} & if\ n_{\Delta H} < n'_{\Delta O} \end{cases}$

The molar flow rate of the hydrogen and the oxygen in the fuel cell is:

$$1 < \gamma_{\mathrm{H-O}} = n_{r\mathrm{H}}\Delta t / n_{r\mathrm{O}}\Delta t < 1.25 \tag{15}$$

i. The actual stock of the hydrogen is calculated by:

$$\begin{cases} n_{rH} = n_{H_2O\_H} + n_{\Delta H} - n_{mhg\_H} \\ n_{rO} = \frac{n_{rH}}{\gamma_{H-O}} \end{cases} \tag{16}$$

ii. The actual stock of the oxygen is calculated by:

$$\begin{cases} n_{rO} = n_{H_2O_O} + n_{\Delta O} - n_{mhg_O} \\ n_{rH} = \gamma_{H-O}n_{rO} \end{cases} \tag{17}$$

The partial pressures of hydrogen and oxygen p_{fc_H}, p_{fc_o} are obtained:

$$\begin{cases} p_{fc\_H} = (\frac{n_{rH}}{N\Delta t} - \frac{dp_{fc\_H}}{dt} \cdot \frac{10^5 V_a}{RT} - \frac{NI_{fc}}{2F})/10^5 K_{H_2} \\ p_{fc\_O} = (\frac{n_{rO}}{N\Delta t} - \frac{dp_{fc\_O}}{dt} \cdot \frac{10^5 V_{ca}}{RT} - \frac{NI_{fc}}{4F})/10^5 K_{O_2} \end{cases} \tag{18}$$

where N is the number of the fuel cell units, V_a and V_{ca} is anode and cathode volumes per unit hydrogen fuel cell respectively, T is the operating temperature of the fuel cell, I_{fc} is the current of the fuel cell, K_{H_2} and K_{O_2} are the molar constant of hydrogen (anode) and oxygen (cathode) respectively.

Based on a fuel cell model, the power of the fuel cell P_{fc} ($P_{fc} \geq 0$) can be obtained:

$$P_{fc} = \begin{cases} P_{fc\_\min} \ , \eta_f \left(U_{fc} \cdot I_{fc}\right) < P_{fc\_\min} \\ \eta_f \left(U_{fc} \cdot I_{fc}\right), \ P_{fc\_\min} \leq \eta_f \left(U_{fc} \cdot I_{fc}\right) \leq P_{fc\_\max} \\ P_{fc\_\max} \ , \eta_f \left(U_{fc} \cdot I_{fc}\right) > P_{fc\_\max} \end{cases} \tag{19}$$

where U_{fc} is the output voltage of the fuel cell, η_f is the power generation efficiency of the fuel cell, $P_{fc\_\max}$ and $P_{fc\_\min}$ are the upper and the lower limits of the fuel cell stack, respectively. Based on double electric layer phenomenon, the output voltage of the hydrogen fuel cell is calculated as follows [31–33]:

$$U_{fc} = N \cdot U_{cell} = N \cdot (E_{nernst} - U_{ohmic} - U_c) \tag{20}$$

where U_{cell} is the output voltage of a single fuel cell, E_{nernst} is the thermodynamic potential, U_{ohmic} is the ohmic polarization overvoltage, and U_c is the equivalent voltage.

The thermodynamic potential can be calculated by Equation (21):

$$E_{nernst} = 1.229 - 8.5 \times 10^{-4}(T - 298.15) + 4.3085 \times 10^{-5} T \times (\ln p_{fc\_H} + 0.5 \ln p_{fc\_O}) \tag{21}$$

The ohmic polarization overvoltage is obtained by:

$$U_{ohmic} = I_{fc}(Z_m + Z_c) = I_{fc}\left(\frac{181.6l[1 + 0.03\frac{I_{fc}}{A} + 0.062(\frac{T}{303})^2(\frac{I_{fc}}{A})^{2.5}]}{A(\varphi - 0.634 - 3\frac{I_{fc}}{A}) \times \exp[4.18(\frac{T-303}{T})]} + Z_c\right) \tag{22}$$

where Z_m is the equivalent membrane impedance; Z_c is the impedance which represents the proton through the exchange membrane; ρ_M is the resistivity; l is the film thickness; A is the activation area of proton exchange membrane; and φ is the proton exchange membrane moisture content. The cell equivalent voltage can be given by:

$$\begin{aligned} U_c = \{&-B \times \ln(1 - \frac{J}{J_{\max}}) - [\varepsilon_1 + \varepsilon_2 T + \varepsilon_3 T \ln(\frac{p_{fc\_O} \times 10^2}{5.08 \times 10^6 \exp(-\frac{498}{T})}) \\ &+ \varepsilon_4 T \ln(I_{fc})]\}(1 - \frac{C}{I_{fc}} \times \frac{dU_c}{dt}) \end{aligned} \tag{23}$$

where B is the equation coefficient; J is the active current density of the cell; $J_{\max}$ is the maximum current density; C is the equivalent capacitance; and ε_1, ε_2, ε_3, ε_4, are the empirical parameters of fuel cell.

(2) If ($P_{re}^{(2)} < 0$) & ($ESOC_S \geq ESOC_{Sa}$) or ($P_{re}^{(1)} < 0$), $ESOC_S$ level is operated within ideal range but the wind power cannot meet the demand. The hydrogen fuel cell discharges to assist wind power with flag1 = 1. n_{rH} and n_{rO} can be obtained by the P_{fc} and then $n_{\Delta H}$ and $n_{\Delta O}$ can be derived.

$$P_{fc} = \begin{cases} P_{fc\_min} \ , \left|P_{re}^i\right| < P_{fc\_\min} \\ \left|P_{re}^i\right| \ , \ P_{fc\_\min} \leq \left|P_{re}^i\right| \leq P_{fc\_\max} \quad i = 1, 2 \\ P_{fc\_\max} \ , \left|P_{re}^i\right| > P_{fc\_\max} \end{cases} \tag{24}$$

The above equation can be simplified as:

$$n_{rH} = \begin{cases} N_{rH\_\min} \times \Delta t, & P_{fc} < P_{fc\_\min} \\ \left|P_{re}^{i}\right| \times \frac{N_{rH\_\max}}{P_{fc\_\max}} \times \Delta t \ , & P_{fc} = \left|P_{re}^{i}\right| \qquad i = 1,\ 2 \\ N_{rH\_\max} \times \Delta t, & P_{fc} > P_{fc\_\max} \end{cases} \tag{25}$$

where $N_{rH\_\min}$ is the flow rate of the hydrogen when the fuel cell operates at minimum power output:

$$n_{rO} = n_{rH}/1.2 \tag{26}$$

(3) If ($P_{re}^{(2)}$ < 0) & ($ESOC_S$ < $ESOC_{Sa}$), or $P_{re}^{(2)} \geq 0$ or $P_{re}^{(3)} \geq 0$, the hydrogen fuel cell suspends with flag1 = 0.

Let $P_{fc} = 0$, $n_{rH} = n_{rO} = 0$, then $n_{\Delta H} = n_{mhg\_H} - n_{H_2O\_H}$, $n_{\Delta O} = n_{mhg\_O} - n_{H_2O\_O}$.
According to the above control rules, the HESS pressure p_{Hre} is obtained:

$$\begin{cases} p_{Hre} = p_{H\_0} + \Delta p_{H\_1} + \Delta p_{H\_2} - \Delta p_{H\_3} - \Delta p_{H\_4} \\ \text{s.t.} \begin{cases} \Delta p_{H\_1} = n_{H_2O\_H} \Delta t \mathrm{RT}_H / \mathrm{V}_{Hcap} \\ \Delta p_{H\_2} = 10^5 k' K_{H_2} p_{fc\_H} \Delta t \mathrm{RT}_H / \mathrm{V}_{Hcap} \\ \Delta p_{H\_3} = n_{mhg} \Delta t \mathrm{RT}_H / \mathrm{V}_{Hcap} \\ \Delta p_{H\_4} = n_{rH} \Delta t \mathrm{RT}_H / \mathrm{V}_{Hcap} \end{cases} \end{cases} \tag{27}$$

where p_{H_0} is the initial pressure of the hydrogen tank; Δp_{H_1} is the pressure increment of the hydrogen caused by water electrolysis; Δp_{H_2} is the pressure increment of the hydrogen caused by incomplete consumption from the fuel cells. Δp_{H_3} is the pressure decrement of the hydrogen caused by methanol production. Δp_{H_4} is the pressure decrement of the hydrogen caused by the fuel cell discharging. k' is the hydrogen recovery rate.

The pressure of the oxygen tank p_{Ore} is calculated by:

$$p_{Ore} = p_{O\_0} + \frac{(n_{H_2O\_O} + 10^5 k' K_{O_2} p_{fc\_O} \Delta t - n_{mhg} - n_{rO}) \mathrm{RT}_O}{\mathrm{V}_{Ocap}} \tag{28}$$

where p_{O_0} is the initial pressure of the oxygen tank.

2.4. Overall Control Scheme

This study is focused on the optimal operation of the hybrid system. When the cluster power is required by the cluster control center, the power from the hybrid system is sent to the grid after the local demand is satisfied. In order to communicate with the cluster control center, a specific indicator "flag2" is used.

By changing flag2, the operation states and the request of the local hybrid system are recorded. The specific actions are as follows:

If P_s + P_{fc} < P_{load} + P_{jh}, flag2 = −1, the local system does not satisfy with the grid plan and the local system requests the cluster control center to provide power assistance;
If P_s + P_{fc} = P_{load} + P_{jh}, flag2 = 0, the local system operates in an ideal state and the established target is realised;
If P_s + P_{fc} > P_{load} + P_{jh}, flag2 = 1, the local system requests assistance from cluster control center and the more power from the local system is sent to the grid.

In order to prevent the amounts of hydrogen and oxygen from reaching their tank limits, an additional control action is developed, as shown in Figure 5.

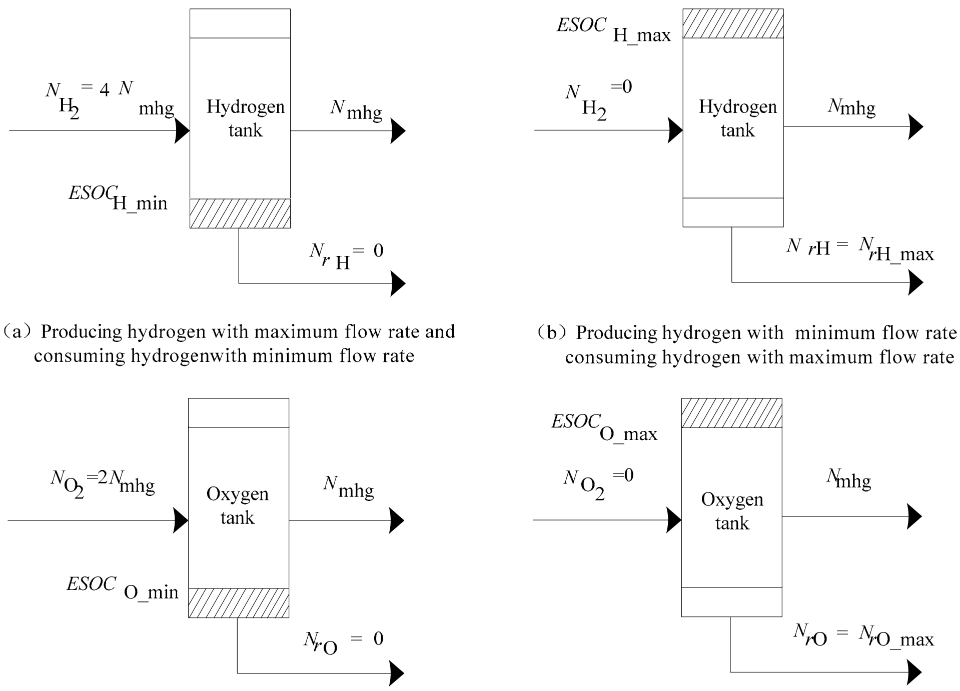

(a) Producing hydrogen with maximum flow rate and consuming hydrogenwith minimum flow rate

(b) Producing hydrogen with minimum flow rate and consuming hydrogen with maximum flow rate

(c) Producing oxygen with maximum flow rate and consuming oxygen with minimum flow rate

(d) Producing oxygen with minimum flow rate and consuming oxygen with maximum flow rate

Figure 5. The extreme cases of hydrogen energy storage system operation.

i. As shown in Figure 5a,c, when $ESOC_H$ or $ESOC_O$ is lower than $ESOC_{H\_min}$ or $ESOC_{O\_min}$, the hybrid system produces the hydrogen/oxygen in maximum and consumes the hydrogen/oxygen in minimum. Δt_a should select the smaller one between Δt_{aH} and Δt_{aO}:

$$\Delta t_a = \begin{cases} \min(\Delta t_{aH}, \Delta t_{aO}) \\ s.t. \begin{cases} \Delta t_{aH} = \frac{(ESOC_{H\_\max} - ESOC_{H\_\min}) p_{Hcap} \mathrm{V}_{Hcap}}{(4N_{mhg} - N_{mhg}) \mathrm{RT}_H} \\ \Delta t_{aO} = \frac{(ESOC_{O\_\max} - ESOC_{O\_\min}) p_{Ocap} \mathrm{V}_{Ocap}}{(2N_{mhg} - N_{mhg}) \mathrm{RT}_O} \end{cases} \end{cases} \tag{29}$$

ii. As shown in Figure 5b,d, when $ESOC_H$ *or* $ESOC_O$ is over than $ESOC_{H\_max}$ or $ESOC_{O\_max}$, the hybrid system produces the hydrogen/oxygen in minimum and consumes hydrogen/oxygen in maximum. Δt_b should select the smaller one between Δt_{bH} and Δt_{bO}:

$$\Delta t_b = \begin{cases} \min(\Delta t_{bH}, \Delta t_{bO}) \\ s.t. \begin{cases} \Delta t_{bH} = \frac{(ESOC_{H\_\max} - ESOC_{H\_\min}) p_{Hcap} \mathrm{V}_{Hcap}}{(N_{mhg} + N_{rH\_\max}) \mathrm{RT}_H} \\ \Delta t_{bO} = \frac{(ESOC_{O\_\max} - ESOC_{O\_\min}) p_{Ocap} \mathrm{V}_{Ocap}}{(N_{mhg} + N_{rH\_\max} / g_{H-O}) \mathrm{RT}_O} \end{cases} \end{cases} \tag{30}$$

Therefore, the time interval Δt is controlled to be:

$$\Delta t < \min(\Delta t_a,\ \Delta t_b) \tag{31}$$

3. Simulation Results

The simulation of a local hybrid system with 10 MW wind power has been carried out by using MATLAB/Simulink. The key parameters of the system are shown in Table 4.

Table 4. Key parameters of the hybrid system.

Parameter	Value	Parameter	Value
U_e	2 V	A	50 cm^2
η_e	80%	φ	14
R	8.3145 J/mol·K	C	3 F
V_{Hcap}	60 m^3	ε_1	−0.9514
V_{Ocap}	60 m^3	ε_2	3.12×10^{-3}
p_{Hcap}	5×10^6 Pa	ε_3	7.4×10^{-5}
p_{Ocap}	5×10^6 Pa	ε_4	-1.87×10^{-4}
p_{H_0}	4.499×10^6 Pa	B	0.016
p_{O_0}	4.499×10^6 Pa	$J_{\max}$	1.2 A/cm^2
T_H	298 K	η_f	90%
T_O	298 K	I_{fc}	25 A
K_{H_2}	6.781×10^{-2} mol/s·atm	V$_a$	0.005 m^3
K_{O_2}	6.781×10^{-2} mol/s·atm	V$_{ca}$	0.01 m^3
k'	0.9	$P_{fc\_\max}$	0.2 MW
N	400	$P_{fc\_\min}$	2×10^{-4} MW
T	350 K	$N_{rH\_\max}$	27,140 mol/s
l	5.1×10^{-3} cm	$N_{rH\_\min}$	1.357 mol/s

In the simulation, $ESOC_{Sa}$ is set 0.31. P_{mhg} and N_{mhg} are set 2.48 MW and 5.134 mol/s respectively. According to Equations (28) and (29), Δt is less than 3.75. Therefore let Δt = 0.5 s. The input and the output power curves are shown in Figures 6 and 7, respectively. The wind power data are from a real 50 MW wind over a 15-h duration. In order to validate the proposed models, the data are scaled down to fit the 10 MW wind turbine model and the time duration is reduced from 15 min to 1 s. $ESOC_S$ exceed the upper limit (0.9) at 11 s as shown in Figure 7, the fuel cell discharges and the $ESOC_S$ reduces. After a control period, $ESOC_S$ restores normal. From 26 s to 27.5 s and from 31.5 s to 34.5 s, the $ESOC_S$ is in the normal range and the storage state is normal. The fuel cells discharge to assist wind power integration, and ensure the output power of the hybrid system to meet the tied-grid demand.

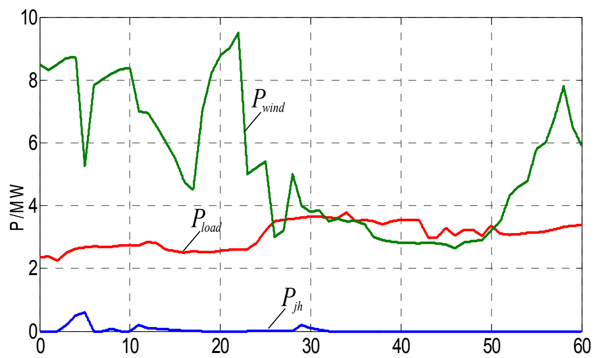

Figure 6. Output power, load and scheduled power curves.

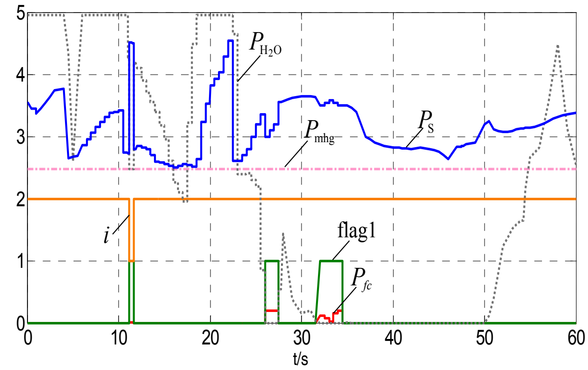

Figure 7. The wind power and the fuel cell power.

Therefore, actual tied-grid power and tied-grid demand curves of the hybrid system are shown as Figure 8.

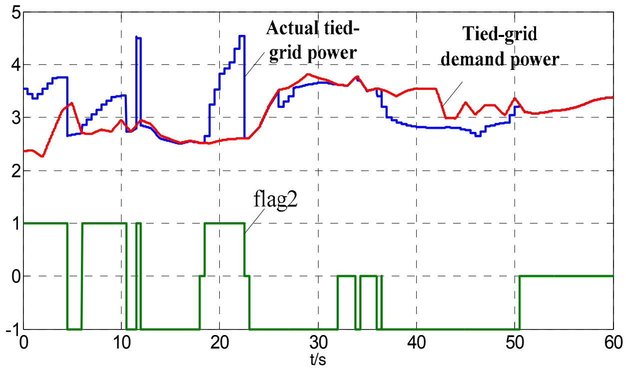

Figure 8. Tied-grid power and overall operation status.

It can be seen from Figure 8 that when actual tied-grid power of the hybrid system does not meet the tied-grid demand, that is $P_s + P_{fc} < P_{load} + P_{jh}$, flag2 is set -1 and the hybrid system requests the cluster center for assistance. Otherwise, flag2 is set 1, the local hybrid system power is excess. If the system power equates the tied-grid demand, the flag2 is set 0. The control objective is achieved. In the above process, the states of the hydrogen/oxygen tanks and HESS are shown in Figures 8–11.

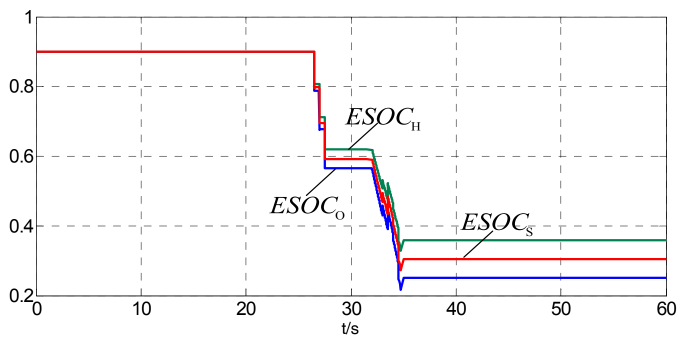

Figure 9. The *ESOC* of the hydrogen tank, oxygen tank and HESS.

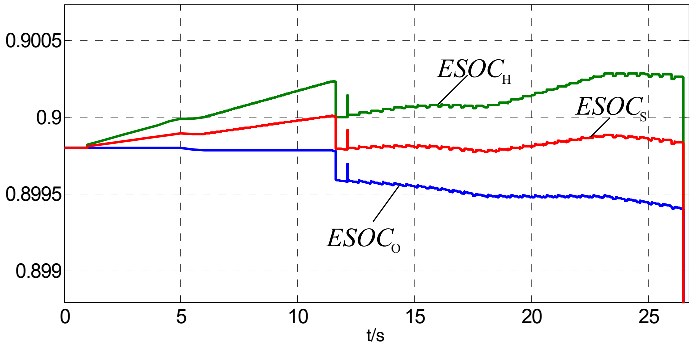

Figure 10. The *ESOC* from 0 s to 26 s.

It can be seen from Figures 9 and 10 that the $ESOC_S$ is in the normal range at the beginning. P_{H_2O} equates $2P_{mhg}$ from 0 s to 4 s and from 6 s to 11 s. The $ESOC_H$ and the $ESOC_S$ rise slowly and the $ESOC_O$ remains unchanged. From 4 s to 6 s, from 11.5 s to 16 s and from 17.5 s to 23 s, $P_{mhg} < P_{H_2O} < 2P_{mhg}$. The $ESOC_H$ and the $ESOC_S$ rise slowly and the $ESOC_O$ decreases slowly. At 11 s, $ESOC_S$ exceeds the upper limit, and the control priority changes. The fuel cells start, and $ESOC_H$, $ESOC_O$ and $ESOC_S$ drop rapidly. The $ESOC_S$ restores to the normal range. From 23 s to 26 s, $P_{H_2O} < P_{mhg}$. The $ESOC_H$, $ESOC_O$ and $ESOC_S$ decrease slowly.

It can be seen from Figure 7 that P_{H_2O} drops rapidly since 26 s. From 26 s to 36 s, P_{H_2O} is less than P_{mhg} and even reduces to zero at 31 s. From 26 s to 27.5 s and from 31 s to 34.5 s, the fuel cells discharge, and the $ESOC_H$, $ESOC_O$ and $ESOC_S$ decrease rapidly as can be seen in Figure 11. From 27.5 s to 31.5 s, the fuel cells suspend and the hydrogen produced by water electrolysis is less than the hydrogen used for coal chemical process. The $ESOC_H$, $ESOC_O$ and $ESOC_S$ decrease slowly. At 34.5 s, $ESOC_S < ESOC_{Sa}$ and the fuel cells suspend. The downward trend of the $ESOC_H$, $ESOC_O$ and $ESOC_S$ has been curbed.

It can be seen from Figures 7 and 12 that $ESOC_{S\_min} < ESOC_S < ESOC_{Sa}$ between 35 s and 60 s while the fuel cells suspend. From 35 s to 50 s, $P_{H_2O} = 0$ and the hydrogen/oxygen for the coal chemical process are provided by the tanks. $ESOC_S$ decreases slowly. From 50 s onwards, P_{H_2O} rises slowly. However, it does not reach $2P_{mhg}$ until 60 s. Therefore, $ESOC_S$ is seen decreasing in this period.

In Figure 13, when the hydrogen for the methanol production is zero, $ESOC_S$ decreases 0.0004 within 15 s. It is at 1 s that $ESOC_S$ decreases from $ESOCs_a$ to $ESOC_{S\_min}$ under unchanged condition. Therefore, let:

$$p_{H\_0} = 1268049.26\mathrm{P}_a \tag{32}$$

and:

$$p_{O\_0} = 732049.26\mathrm{P}_a \tag{33}$$

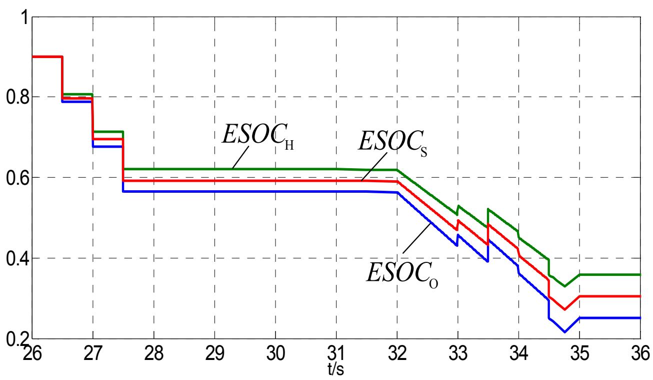

Figure 11. The *ESOC* from 26 s to 35 s.

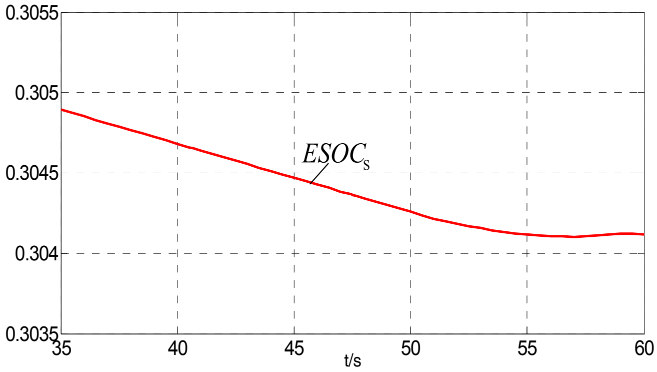

Figure 12. The *ESOC* from 35 s to 60 s.

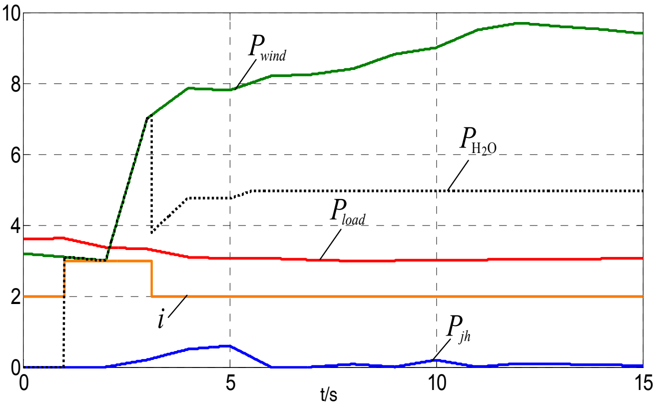

Figure 13. The power and the flag bit curve beyond lower limit.

The simulations when $ESOC_S$ below the low limit is carried out based on this model. The hydrogen tank and the *ESOC* of the HESS are shown in Figures 14 and 15. In Figures 14 and 15, the $ESOC_S$ reach the lower limit and the control priority changes. The wind power is used for the water electrolysis at 1 s. The $ESOC_S$ recovers to the normal range at 3 s. After that, the power for the water electrolysis increases and maintains $2P_{mhg}$ until 5.5 s. The $ESOC_H$, $ESOC_O$ and $ESOC_S$ increase slowly.

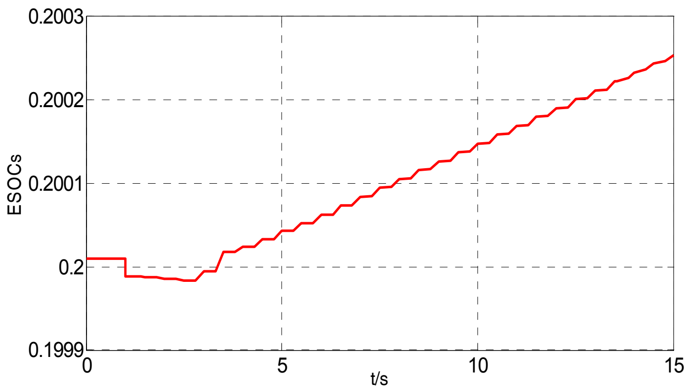

Figure 14. The curve of the *ESOC*s below the low limit.

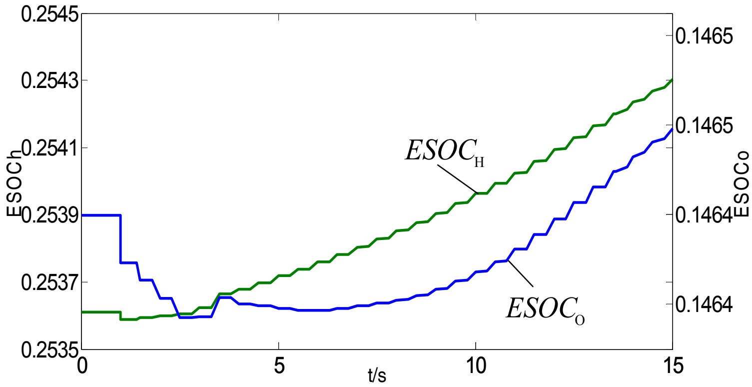

Figure 15. The curve of the $ESOC_H$ and $ESOC_O$ below the low limit.

4. Conclusions

This paper has presented a new hybrid system involving wind turbines, hydrogen energy storage, water electrolyser, and fuel cells. The novelty lies in the coordinated control scheme to maximize the utilisation of wind power with a constant methanol output whilst still reducing CO_2 emissions. All the symbols used in the paper can refer to Table A1 in Appendix A. The main contributions of the study can be concluded as follows:

(1) This work takes advantage of wind power for electricity generation and for energy storage. In addition, coal-based energy systems for methanol production in a cleaner manner. This is critically important for China as well as many coal-dependent economies.
(2) It integrates some interdisciplinary techniques into a multi-functional dynamic system to effectively manage various energy sources to enhance stable power supply stability, increase energy efficiency in utilization, and reduce CO_2 emissions.
(3) It proposes a concept prototype and then implements the structured system in a simulation environment, which significantly reduces the real test cost.
(4) The simulation results have confirmed the technical feasibility of the proposed system. It paves the way for next stage progression in small scale real tests and future commercialization of the technology.
(5) Because of the optimal design and control of the hybrid system, energy efficiency and cost efficiency will be improved. This has a significant economic implications. Moreover, the reduction in CO_2 emissions will have an additional benefit from Carbon Trading Scheme in China.

As this is just a theoretical study in pioneering stage in China, there are several pertinent aspects need to be fully investigated before real system implementation and applications. These are:

(1) Development of a full-scale simulation with hardware-in-loop real-time simulator for feasibility investigation.
(2) Development of a full scale demonstration experimental setup of the system.
(3) Conduction economic analysis, costs and gains, energy trading and carbon trading.
(4) Carrying out a study on other social, environmental, legal impacts to minimize the uptake of the proposed technology.

Acknowledgments: This research is supported by National Natural Science Foundation of China (NSFC 51367018, 51321005) and Xinjiang Science Foundation for Distinguished Young Scholars (2014711005).

Author Contributions: In this article, T. Yuan and Q. Duan conceived and designed the system; J. Hu and X. Yuan performed the experiments; Q. Zhu built the simulation models; X. Chen and W. Cao analysed data and wrote the paper.

Conflicts of Interest: The authors declare no conflict of interest.

Appendix A

Table A1. Symbols.

1	A	Active area of the membrane
2	B	Equation coefficient
3	C	Equivalent capacitor of fuel cell
4	E_{nernst}	Thermodynamic potential
5	$ESOC$	Equivalent state of charge
6	$ESOC_H$	Equivalent state of charge of the hydrogen tank
7	$ESOC_S$	Equivalent state of charge of the *HESS*
8	$ESOC_{S_a}$	Threshold of *ESOC*
9	$ESOC_O$	Equivalent state of charge of the oxygen tank
10	$ESOC_{X\_\max}$	The upper limit of the *ESOC*
11	$ESOC_{X\_\min}$	The low limit of the *ESOC*
12	F	Faraday constant
13	I_e	Current in water electrolyser
14	I_{fc}	Discharge current of fuel cell
15	J	ampere density in fuel cell
16	$J_{\max}$	Maximum ampere density in fuel cell
17	k'	Fuel recovery rate
18	k_{H_2}	Hydrogen constant
19	K_{O_2}	Oxygen constant
20	l	Thickness of the membrane
21	M_W	Nominal capacity of the wind farm
22	$n_{H_2O\_H}$	Hydrogen production amount by water electrolysis in Δt
23	$n_{H_2O\_O}$	Oxygen production amount by water electrolysis in Δt
24	n_{mhg_H}	Hydrogen consumption by methanol production in Δt
25	n_{mhg_O}	Oxygen consumption by methanol production in Δt
26	n_{rH}	Hydrogen consumption by fuel cell in Δt
27	n_{rO}	Oxygen consumption by fuel cell in Δt
28	$n_{\Delta H}$	Hydrogen consumption amount in Δt
29	$n_{\Delta O}$	Oxygen consumption in Δt
30	$n'_{\Delta H}$	Hydrogen amount when the pressure of the hydrogen tank is over the upper limit
31	$n'_{\Delta O}$	Oxygen amount when the pressure of the oxygen tank is over the upper limit
32	N_e	The serial units of fuel cells
33	N_{fc}	Flow rate of the hydrogen fed in the fuel cells
34	N_{H_2}	Hydrogen flow rate in water electrolysis
35	N_{H_2O}	Flow rate of the hydrogen by water electrolysis
36	N_{mhg}	Hydrogen flow rate consumed by methanol production at the rated power
37	$N_{rH\_\max}$	Hydrogen consumption at full discharging of the fuel cells
38	$N_{rH\_\min}$	Hydrogen flow rate when fuel cell discharging in minimum
39	p_{cap}	Tank pressure when fully charged
40	p_{fc_H}	Hydrogen pressure in a fuel cell
41	$p_{fc\_\max}$	Maximum power output of fuel cell discharging
42	$p_{fc\_\min}$	Minimum power output of fuel cell discharging
43	p_{fc_O}	Oxygen pressure in a fuel cell
44	p_{Hcap}	Full pressure of the hydrogen tank
45	p_{Hre}	Current pressure in the hydrogen tank
46	p_{H_0}	Initial pressure in hydrogen tank
47	p_{Ocap}	Full pressure of the oxygen tank
48	p_{Ore}	Current pressure in the oxygen tank
49	p_{O_0}	Initial pressure in oxygen tank
50	p_{vre}	Current pressure in storage tank
51	P_{fc}	Discharging power of fuel cell
52	P_{H_2O}	Power for water electrolysis
53	P_{jh}	Cluster power demand dispatched by cluster control center

Table A1. *Cont.*

54	P_{load}	Local power demand
55	P_{mhg}	Equivalent power for the water electrolysis when the amount of the hydrogen production is equal to the amount of methanol production
56	P_S	Fed-in power to the grid
57	P_{wind}	Wind power
58	R	Idea fuel constant (8.3145 J/mol·K)
59	T	Nominal temperature of fuel cell
60	T_H	Temperature in hydrogen tank
61	T_O	Temperature in oxygen tank
62	U_c	Equivalent voltage
63	U_{cell}	Output voltage of a single fuel cell
64	U_{fc}	Discharging voltage of fuel cell
65	U_{ohmic}	Polarization voltage
66	V_{Hcap}	Volume capacity of the hydrogen tank
67	V_{Ocap}	Volume capacity of the oxygen tank
68	V_a	Size of a single fuel cell
69	V_{ca}	Cathode size of a single fuel cell
70	V_m	Molar volume
71	Z_m	Equivalent resistance of the membrane
72	Z_c	Equivalent resistance of a fuel cell
73	$\varepsilon_1, \varepsilon_2, \varepsilon_3, \varepsilon_4$	Empirical coefficients
74	η_e	Efficiency of water electrolyser
75	η_f	Discharging efficiency of fuel cell
76	ρ_M	Resistant rate of the membrane
77	φ	Water rate of the membrane
78	Δp_{H_1}	Hydrogen pressure increment by water electrolysis
79	Δp_{H_2}	Hydrogen pressure increment by incomplete consumption by fuel cell
80	Δp_{H_3}	Hydrogen pressure decrement by methanol production
81	Δp_{H_4}	Hydrogen pressure decrement by fuel cell consumption
82	Δt	Operational time interval

References

1. Shu, Y.B. Deepening Cooperation, Embrace Challenges to Promote Sustainable Development of Renewable Energy. In Proceedings of the 2017 International Conference on Renewable Energy Development and Technology and High-Level Dialogue, Frankfurt, Germany, 16 June 2017; Available online: http://www.epri.sgcc.com.cn/html/eprien/col2016201124/2017-07/03/20170703161018331376621_1.html (accessed on 10 July 2017).
2. Zhao, H.; Wu, Q.; Hu, S.; Xu, H. Review of energy storage system for wind power integration support. *Appl. Energy* **2015**, *137*, 545–553. [CrossRef]
3. Perera, A.; Vahid, M.; Mauree, D.; Scartezzini, J. Electrical hubs: An effective way to integrate non-dispatchable renewable energy sources with minimum impact to the grid. *Appl. Energy* **2017**, *190*, 232–248. [CrossRef]
4. Solomon, A.; Kammen, D.; Callaway, D. Investigating the impact of wind–solar complementarities on energy storage requirement and the corresponding supply reliability criteria. *Appl. Energy* **2016**, *168*, 130–145. [CrossRef]
5. Shi, J.; Tang, Y.J.; Ren, L.; Li, J.D. Application of SMES in wind farm to improve voltage stability. *Phys. C Supercond. Appl.* **2008**, *15*, 2100–2103. [CrossRef]
6. Li, N.; Zhang, X.L.; Shi, M.J.; Zhou, S.L. The prospects of China's long-term economic development and CO_2 emissions under fossil fuel supply constraints. *Resour. Conserv. Recycl.* **2017**, *121*, 11–22. [CrossRef]
7. Shekhar, C.C. Methanol: The New Hydrogen, MIT Technology Review. Available online: https://www.technologyreview.com/s/405597/methanol-the-new-hydrogen/ (accessed on 10 July 2017).
8. Li, Q.; Wei, Y.N.; Chen, Z.A. Water-CCUS nexus: Challenges and opportunities of China's coal chemical industry. *Clean Technol. Environ. Policy* **2016**, *18*, 775–786. [CrossRef]
9. Khaitan, S.K.; Raju, M.; McCalley, J.D. Design of a novel and efficient hydrogen compressor for wind energy based storage systems. *Int. J. Hydrog. Energy* **2015**, *40*, 1379–1387. [CrossRef]

10. Lotfy, M.E.; Senjyu, T.; Farahat, M.A.; Abdel-Gawad, A.F.; Yona, A. A frequency control approach for hybrid power system using multi-objective optimization. *Energies* **2017**, *10*, 80. [CrossRef]
11. Maleki, A.; Hafeznia, H.; Rosen, M.A.; Pourfayaz, F. Optimization of a grid-connected hybrid solar-wind-hydrogen CHP system for residential applications by efficient metaheuristic approaches. *Appl. Therm. Eng.* **2017**, *123*, 1263–1277. [CrossRef]
12. Beccali, M.; Brunone, S.; Finocchiaro, P. Method for size optimisation of large wind–hydrogen systems with high penetration on power grids. *Appl. Energy* **2013**, *102*, 534–544. [CrossRef]
13. Chrenko, D.; Lecoq, S.; Herail, E. Static and dynamic modeling of a diesel fed fuel cell power supply. *Int. J. Hydrog. Energy* **2010**, *35*, 1377–1389. [CrossRef]
14. Boulon, L.; Agbossou, K.; Hissel, D. A macroscopic PEM fuel cell model including water phenomena for vehicle simulation. *Renew. Energy* **2012**, *46*, 81–91. [CrossRef]
15. Jiang, Z.H.; Yu, X.W. Modeling and control of an integrated wind power generation and energy storage system. In Proceedings of the Power & Energy Society General Meeting 2009, Calgary, AB, Canada, 26–30 July 2009; pp. 1–8.
16. Abbey, C.; Joos, G. Supercapacitor Energy Storage for Wind Energy Applications. *IEEE Trans. Ind. Appl.* **2007**, *43*, 769–776. [CrossRef]
17. Ni, W.D.; Gao, J.; Chen, Z.; Li, Z. How to make the production of Methanol/DME "GREENER"—The integration of wind power with coal chemical industry. *Front. Energy Power Eng.* **2009**, *3*, 94–98. (In Chinese) [CrossRef]
18. Yuan, T.; Lin, K.; Guan, Y.; Dong, X.; Sun, Y.; Mei, S. Modeling on hydrogen producing progress in EMR based wind power-hydrogen energy storage and coal chemical pluripotent coupling system. *High Volt. Eng.* **2015**, *41*, 2156–2164. (In Chinese)
19. Elgammal, A.A.A.; El-naggar, M.F. MOPSO-based optimal control of shunt active power filter using a variable structure fuzzy logic sliding mode controller for hybrid (FC-PV-Wind-Battery) energy utilisation scheme. *IET Renew. Power Gener.* **2017**, *11*, 1148–1156. [CrossRef]
20. Saravanan, S.; Thangavel, S. Instantaneous reference current scheme based power management system for a solar/wind/fuel cell fed hybrid power supply. *Int. J. Electr. Power Energy Syst.* **2014**, *55*, 155–170. [CrossRef]
21. Mohammadi, S.; Soleymani, S.; Mozafari, B. Scenario-based stochastic operation management of MicroGrid including Wind, Photovoltaic, Micro-Turbine, Fuel Cell and Energy Storage Devices. *Int. J. Electr. Power Energy Syst.* **2014**, *54*, 525–535. [CrossRef]
22. Xu, L.J.; Fan, X.C.; Wang, W.Q. Renewable and sustainable energy of Xinjiang and development strategy of node areas in the "Silk Road Economic Belt". *Renew. Sustain. Energy Rev.* **2017**, *79*, 274–285. [CrossRef]
23. National Energy Administration, Chinese. Energy Development 12th Five-Year Plan. Available online: http://www.nea.gov.cn/2013-01/28/c_132132808.htm# (accessed on 1 January 2013).
24. Xinhua. China Tops the World in Renewable Energy Production: BP Report. Available online: http://news.xinhuanet.com/english/2017-07/10/c_136432582.htm (accessed on 10 July 2017).
25. Lin, H.; Jin, H.G.; Gao, L.; Han, W. Economic analysis of coal-based polygeneration system for methanol and power production. *Energy* **2010**, *35*, 858–863. [CrossRef]
26. Tang, L.; Wu, J.Q.; Yu, L.; Bao, Q. Carbon emissions trading scheme exploration in China: A multi-agent-based model. *Energy Policy* **2015**, *81*, 152–169. [CrossRef]
27. Jia, L.; Qu, F.C. Index of Carbon Dioxide and the Main Pollutant Emissions of Coal Chemical Industry Demonstration Project Research. *Chem. Ind.* **2014**, *7*, 13–17. (In Chinese)
28. Lamy, C. From hydrogen production by water electrolysis to its utilization in a PEM fuel cell or in a SO fuel cell: Some considerations on the energy efficiencies. *Int. J. Hydrog. Energy* **2016**, *41*, 15415–15425. [CrossRef]
29. Giaconia, A.; Grena, R.; Lanchi, M.; Liberatore, R.; Tarquini, P. Hydrogen/methanol production by sulfur–iodine thermochemical cycle powered by combined solar/fossil energy. *Int. J. Hydrog. Energy* **2007**, *32*, 469–481. [CrossRef]
30. Wang, W.L.; Wang, D.; Jia, H.J.; He, G.X.; Hu, Q.; Sui, P.C.; Fan, M.H. Performance Evaluation of a Hydrogen-Based Clean Energy Hub with Electrolyzers as a Self-Regulating Demand Response Management Mechanism. *Energies* **2017**, *10*, 1211. [CrossRef]
31. Francois, B.; Hissel, D.; Iqbal, M.T. Dynamic Modelling of a Fuel Cell and Wind Turbine DC-Linked Power System. In Proceedings of the ELECTRIMACS Conference, Hammamet, Tunisia, 17–20 April 2005; The ELECTRIMACS Technical Committee: Hammamet, Tunisia, 2005.

32. Choi, S.; Chu, K.; Ryu, J.; Sunwoo, M. Empirical modeling of a polymer electrolyte fuel cell based on water transport investigation and current interrupt measurement. *Int. J. Automot. Technol.* **2009**, *10*, 719–732. [CrossRef]
33. Mann, R.F.; Amphlett, J.C.; Hooper, M.A.I.; Jensen, H.M.; Peppley, B.A.; Roberge, P.R. Development and application of a generalised steady-state electrochemical model for a PEM fuel cell. *J. Power Sources* **2000**, *86*, 173–180. [CrossRef]